Süleyman Demirel Üniversitesi
Fen Bilimleri Enstitüsü Dergisi
Cilt 29, Sayı 3, 675-683, 2025

Süleyman Demirel University
Journal of Natural and Applied Sciences
Volume 29, Issue 3, 675-683, 2025

DOI: 10.19113/sdufenbed.1798410

Quantification of Amine Groups in Aminopropyltrimethoxysilane-Functionalized Silica Nanoparticles: Synthesis, Size Control, and Application as Sorbents for Rare Earth Metals

Seda DEMİREL TOPEL[1*]

1Antalya Bilim University, Faculty of Engineering and Natural Sciences, Department of Electrical and Electronics Engineering, 07190, Döşemealtı, Türkiye

(Alınış / Received: 06.10.2025, Kabul / Accepted: 18.12.2025, Online Yayınlanma / Published Online: 25.12.2025)

Keywords
Silica nanoparticles,
Quantification,
Organosilane,
Spectroscopy,
Rare Earth Element

Abstract: SiO_2 nanoparticles were prepared using the Stöber method under different variable factors, such as concentration of tetraethyl orthosilicate, ammonia, and temperature, which yielded tunable sizes, and accordingly, 3-aminopropyltrimethoxysilane (APTMS) was grafted onto the silica surface to yield SiO_2-APTMS nanoparticles. FTIR, TGA, and XPS confirmed the grafting of aminopropyl groups, while quantitative analysis was carried out using both the ninhydrin assay and thermogravimetric measurements. Ninhydrin selectively revealed the presence of accessible surface amines, whereas TGA provided the total organic loading, with calculated grafting densities ranging from 3.4 to 9.6 molecules.nm^{-2}. The functionalized SiO_2–APTMS nanoparticles were further examined as sorbent materials for rare earth elements (La^{3+}, Nd^{3+}, Dy^{3+}, Er^{3+}). Adsorption studies demonstrated a rapid uptake within 100 min and reached an equilibrium at ~200 min. Dy^{3+} exhibited the highest capacity (~0.63 mmol·g^{-1}) among those elements. The results demonstrated the successful surface modification and quantification of aminopropyl groups, as well as the promising potential of SiO_2–APTMS nanoparticles for rare earth recovery from aqueous solutions.

Aminopropiltrimetoksisilan ile Fonksiyonelleştirilmiş Silika Nanoparçacıklarındaki Amin Gruplarının Kuantifikasyonu: Sentez, Boyut Kontrolü ve Nadir Toprak Metalleri için Sorbent Olarak Uygulaması

Anahtar Kelimeler
Silika nanoparçacıklar,
Kuantifikasyon,
Organosilan,
Spektroskopi,
Nadir Toprak Elementi

Öz: SiO_2 nanopartikülleri, tetraetil ortosilikat konsantrasyonu, amonyak ve sıcaklık gibi farklı değişken koşullar altında Stöber yöntemi kullanılarak sentezlendi ve bu sayede ayarlanabilir boyutlar elde edildi. Ardından, 3-aminopropiltrimetoksi silan (APTMS) silika yüzeyine aşılanarak SiO_2–APTMS nanopartikülleri oluşturuldu. FTIR, TGA ve XPS analizleri, aminopropil gruplarının yüzeye başarıyla aşılandığını doğruladı. Kantitatif analizler ise hem ninhidrin testi hem de termogravimetrik ölçümlerle gerçekleştirildi. Ninhidrin testi, yüzeydeki erişilebilir amin gruplarını seçici bir şekilde ortaya koyarken; TGA, 3,4 ila 9,6 molekül·nm^{-2} arasında değişen aşılanma yoğunluklarıyla toplam organik yüklemeyi belirledi. Fonksiyonelleştirilmiş SiO_2–APTMS nanopartikülleri, nadir toprak elementleri (La^{3+}, Nd^{3+}, Dy^{3+}, Er^{3+}) için adsorban malzemeler olarak daha ayrıntılı biçimde incelendi. Adsorpsiyon deneyleri, 100 dakika içinde hızlı bir emilim gerçekleştiğini ve yaklaşık 200 dakikada dengeye ulaşıldığını gösterdi. Bu elementler arasında Dy^{3+} en yüksek adsorpsiyon kapasitesine (~0,63 mmol·g^{-1}) sahip olduğu gözlendi. Sonuçlar, aminopropil gruplarının başarılı şekilde yüzeye aşılandığını ve miktarının doğrulandığını gösterdi. Ayrıca, SiO_2–APTMS nanopartiküllerinin sulu çözeltilerden nadir toprak elementlerinin geri kazanımı için umut verici bir potansiyele sahip olduğu ortaya kondu.

*Corresponding author: seda.demireltopel@antalya.edu.tr

1. Introduction

Silica nanoparticles have found applications in various fields, including drug delivery, catalysis, and environmental remediation, due to their tunable size, high surface area, and excellent biocompatibility [1]. Simple surface modification, particularly with silanes containing primary amine groups, such as 3-aminopropyltriethoxy silane, further enhances their applicability by providing affinity for biomolecules or ions through alterations in surface charge [2]. This surface modification, which is critical for optimizing the performance of nanoparticles in environmental applications, is typically accomplished by using aminopropyltriethoxy silane (APTES) or aminopropyltrimethoxy silane (APTMS) [3]. Accurate quantification of these amine groups is essential for quality control, comprehending reaction kinetics, and ensuring reproducible performance across a range of applications. Despite their significance, there is a notable gap in the literature regarding standardized and highly accurate methodologies for the quantitative assessment of amine functionalities on silica nanoparticle surfaces. This challenge is further compounded by the inherent heterogeneity in amine content arising from the functionalization process itself, which can range from monolayer coverage to multilayer amine modifications [4]. For example, the formation of localized regions of amine multilayers or amination of internal pores can lead to inaccessible amine groups that are difficult to quantify by conventional colorimetric assays [5]. Therefore, these methods should be supplemented by spectroscopic and thermal analysis methods [6]. A robust and comprehensive analysis approach is needed to accurately identify both total and accessible amine content, enabling reliable characterization of these versatile nanomaterials.

On the other hand, amine-functionalized silica nanoparticles have been tailored for the removal of rare earth ions from aqueous solutions. These critical elements are widely used in permanent batteries, energy-efficient materials, optical devices, and advanced electronics [7]. Since the isolation of rare earth elements from their reservoirs often involves energy loss, high cost, and the use of hazardous chemicals, the development of efficient removal strategies for these elements from wastewater through adsorption-based approaches is of great importance [8]. Therefore, the design and preparation of nanosorbents with high surface area and proper functional groups has gained interest in sequestrating these ions. For example, Hu et al. reported the synthesis of tetradentate phenylenedioxy diamide (PDDA) ligands, which were immobilized onto large-pore, three-dimensional KIT-6 mesoporous silica [9]. When applied in solid-phase extraction, these hybrid sorbents allowed size-selective separation of rare earth elements, governed by the bite angles of the ligands. Ramasamy et al. functionalized the micron-sized silica gels with 3-Aminopropyl triethoxysilane (APTES), 3-Aminopropyl trimethoxysilane (APTMS), Trimethoxymethylsilane (MTM), and Chlorotrimethylsilane, and obtained that APTES/APTMS silica gels yielded the most impressive behavior among the four adsorbents in all the cases [10]. In addition, Vardanyan et al. synthesized amine and sulfur-containing SiO_2 nanoparticles by the grafting method and investigated their sorption behavior towards Nd^{3+}, Sm^{3+} as rare earth, and Ni^{2+} and Co^{2+} as late transitions, and showed high sorption capacities between 0.5-1.8 mmol/g [11].

This work addresses the production of silica nanoparticles grafted with APTMS for use in the isolation of rare earth ions such as dysprosium (Dy^{3+}), neodymium (Nd^{3+}), erbium (Er^{3+}), and lanthanum (La^{3+}) ions from aqueous solutions. The amine-grafted nanosorbent was investigated for its sorption behavior toward those ions as well as their physical and chemical characteristics. Consequently, it is essential to precisely determine the amine groups on the surface to predict and improve the sequestration effectiveness of functionalized silica nanoparticles. Here, APTMS-functionalized silica nanoparticles were investigated for their potential as a sorbent material to explore the affinity of rare earth ions.

2. Materials and Method

3-aminopropyltrimethoxysilane (code: SIA0610.1) was purchased from Gelest, USA. Tetraethyl orthosilicate (TEOS), ammonium hydroxide (NH_4OH), sodium hydroxide (NaOH), hydrochloric acid (%37), toluene, methanol, and ethanol were purchased from Sigma-Aldrich. Toluene was dried over calcium hydride (CaH_2). Methanol and ethanol were used without any purification.

2.1 Synthesis of unmodified silica nanoparticles

A Stöber method has been carried out for the synthesis of silica nanoparticles [12]. In this method, ethanol, distilled water, and ammonium hydroxide (NH_4OH) as a catalyst were mixed in a two-necked round-bottom flask and heated to a specified temperature (Table 1). The concentrations of water and ammonia were calculated according to Table 1. Later, the TEOS was added dropwise to the initial solution at the specified temperature and stirred at 1500 rpm for 24 hours. After that, the SiO_2 nanoparticles were separated at 12.000 rpm using an ultracentrifuge. The nanoparticles were washed with ethanol: distilled water (1:1) (50 mL) for 3 times, then dried in a vacuum oven at 40°C.

2.2 Synthesis of APTMS-modified silica nanoparticles

The SiO_2 nanoparticles (1.00 g) were dispersed in anhydrous toluene (100 mL). The APTMS (1.5 mL)

was introduced to the first solution under a nitrogen gas atmosphere and heated to 80°C overnight. After that, the ligand-bonded nanoparticles were washed one time with toluene to remove unbonded ligand, and washing continued for three times with 50 mL of ethanol: water (1:1). The solution was centrifuged at 10.000 rpm for 15 min. The ligand-grafted SiO_2 nanoparticles were dried in a vacuum oven at 40°C.

2.3 Quantification of the amine groups using the ninhydrin colorimetric assay

The ninhydrin solution, consisting of 2% ninhydrin in ethanol, was used to detect amine groups [13]. A quantity of 6.6 mg of SiO_2-APTMS was dispersed in 5 mL of ethanol, and 100 µL of ninhydrin solution was added. The mixture was heated to 90 °C and stirred for 90 minutes until it changed color to a deep blue-purple, as shown in Figure 1. After cooling to room temperature, the mixture was centrifuged at 12.000 rpm for 15 minutes, and the UV-Vis spectrometer was used to analyze the supernatant [14]. To determine the unknown concentration of amine in SiO_2-APTMS, a calibration curve of hexylamine has been plotted. According to those various concentrations of hexylamine, including 0.2 mM, 0.4 mM, 0.6 mM, 0.8 mM, and 1 mM, were mixed with 5 mL of ethanol (Figure 1A). Ninhydrin solution (100 µL) was added to each of these solutions, which were then heated to 90 °C and stirred for 90 minutes until a deep blue-purple color was observed, as indicated in Figure 1B. The maximum intensities of the absorbances at 580 nm (λ_{max}) were measured using a UV-Vis spectrometer (Figure 1A). A blank experiment was conducted using the same procedure for bare SiO_2 nanoparticles, but no change in color was detected (Figure 1B)

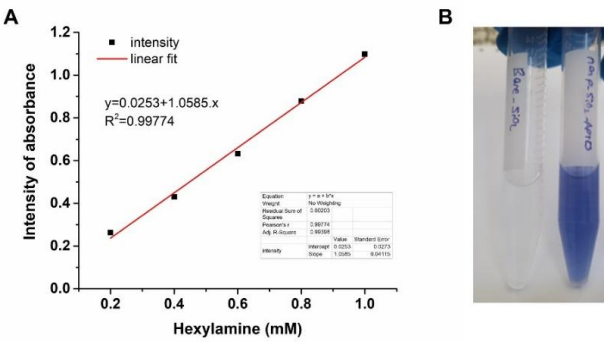

Figure 1. Calibration curve of hexylamine solution in ethanol **(A)**, Comparison of the ninhydrin test between bare and APTMS-linked SiO_2 NPs **(B)**

The molar quantification of amine groups (MQA, mol/g) grafted onto the surface of SiO_2-APTMS is determined relative to the weight of the nanoparticles, according to equation 1. In this equation, M is the concentration of amine group (mol/L); V is the volume (L), and W_s is the amount of SiO_2-APTMS (g).

$$MQA\ (mol/g) = \frac{M.V}{W_s} \quad (1)$$

An alternative measure of amine grafting is expressed in equation 2, representing the number of amine molecules ($NAM,\ molecules/nm^2$) attached to the surface of SiO_2-APTMS, calculated with respect to their surface area [15].

$$NAM(molecule/nm^2) = \frac{MQA}{S_{BET}}\ x\ 6.022\ x\ 10^5 \quad (2)$$

$S_{BET}\ (m^2/g)$ denotes the specific surface area of SiO_2-APTMS. The weight fraction of the aminopropyl groups $(W_{ap},\ \%)$ on the nanoparticles is determined using equation 3.

$$W_{ap}\ (\%) = (MQA\ x\ M_{ap})x\ 100 \quad (3)$$

M_{ap} represents the molar mass of the amine group grafted onto the silica surface. Accordingly, the grafted APTMS molecules immobilized on the surface of SiO_2-APTMS are expressed in equation 4 [15]. The initial molar amount of APTMS is denoted as $n_{initial}\ (mol)$, and $W_{SiO2\ NPs}$ is the weight of the initial amount of SiO_2 nanoparticles before grafting APTMS.

$$Grafting\ ratio\ (\%) = \frac{MQA\ x\ W_{SiO2-APTMS}}{n_{initial}}\ x\ 100 \quad (4)$$

2.4 Characterization

The morphology and size distribution of the SiO_2 nanoparticles were characterized using a transmission electron microscope (TEM, Jeol JEM-2200FS). For sample preparation, 1 mg/mL of the nanosorbent was dispersed in ethanol, and a small amount of the dispersion was deposited onto a carbon-coated copper grid. After allowing the solvent to evaporate completely, TEM images were captured to analyze the nanosorbent's structural features and size distribution. The size distribution of the SiO_2 nanoparticles was analysed using dynamic light scattering (DLS), Malvern, Panalytical. The SiO_2 powder was milled using an agate mortar.

3. Results and Discussion

3.1 TEM and DLS analysis of the SiO_2 nanoparticles

According to TEM images, the particle sizes of SiO2 nanoparticles for samples 1, 2, and 3 obtained from

the reaction conditions 1, 2, and 3 in Table 1 were determined as 11.9 ± 1.4 nm, 110.9 ± 1.1 nm, and 41.1 ± 4.4 nm, respectively (Table 1, Figure 2).

Table 1. Experimental conditions for the synthesis of non-porous SiO_2 particles

No	[TEOS] *(M)*	H_2O/ TEOS	[NH_3] *(M)*	Temp. *(°C)*	TEM Particle size *(nm)*	DLS Filtered *(nm)*	DLS Non-filt *(nm)*	PdI Filt.	PdI Non-filt.
1	0.40	60	0.10	65	11.9 ± 1.4	289	344	1.04	0.71
2	0.25	50	0.18	65	110.9 ± 1.1	171.9	204.4	0.66	2.31
3	0.35	50	0.10	55	41.1 ± 4.4	204.4	289	4482	11.7

At higher TEOS concentration (0.40 M) with 0.10 M NH_3 at 65 °C, small spherical particles with an average size of 11.9 ± 1.4 nm were obtained, indicating rapid nucleation (Figure 2 A1 and A2). When the ammonia concentration was raised to 0.18 M (0.25 M TEOS, 65 °C), the particles grew much larger, with an average size of 110.9 ± 1.1 nm (Figure 2 B1 and B2). When the reaction temperature was lowered to 55 °C (0.35 M TEOS, 0.10 M NH_3), nanoparticles of medium size with an average size of 41.1 ± 4.4 nm were seen (Figure 2 C1 and C2).

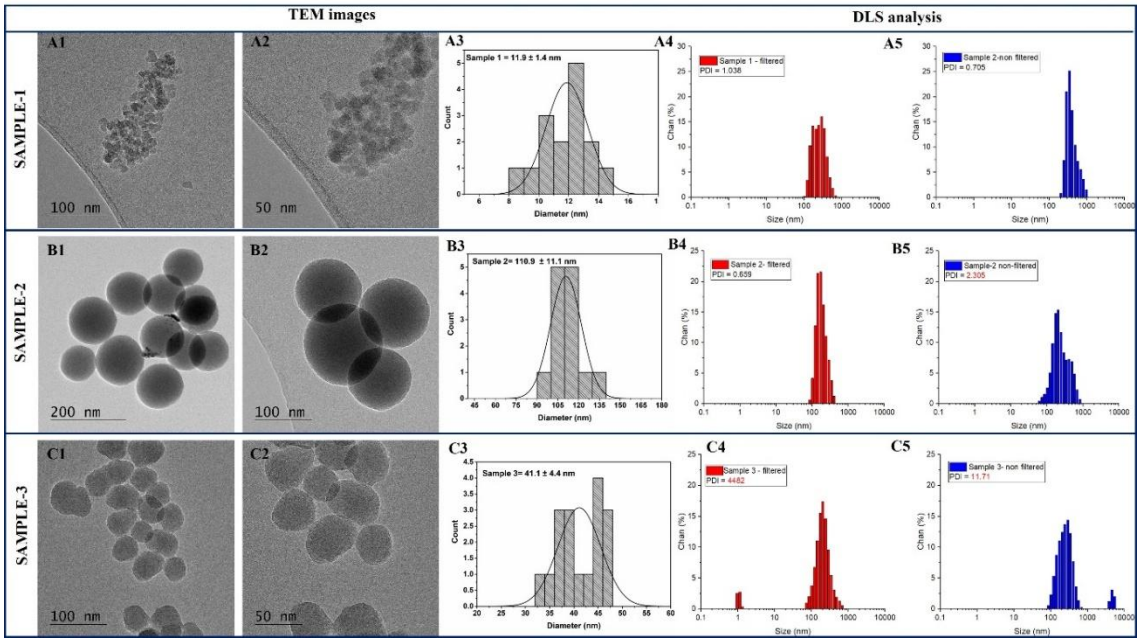

Figure 2. TEM images of SiO_2 nanoparticles prepared at different conditions (A-C,1-3) and their DLS analysis using filtration and without filtration (A-C, 4-5)

The lower thermal energy slowed the growth kinetics; thus, the particles were larger than those in Condition 1 but smaller and less uniform than those in Condition 2. Additionally, we conducted DLS measurements and recorded the average size as well as the polydispersity index (PdI) values. DLS consistently reported larger hydrodynamic diameters than TEM, reflecting the hydration shell and degree of aggregation in suspension. In Condition 1, the hydrodynamic size increased to 289 nm (filtered) and 344 nm (non-filtered), much larger than the TEM size (~12 nm), demonstrating strong aggregation of very small primary particles (Table 1, Figure 2 A3-A5). Condition 2 showed smaller DLS values of 171.9 nm (filtered) and 204.4 nm (non-filtered), which are much closer to the TEM size (~111 nm), indicating reduced aggregation and improved colloidal stability (Table 1, (Table 1, Figure 2 B3-B5). Condition 3 resulted in 204.4 nm (filtered) and 289 nm (non-filtered), still considerably larger than the TEM values, reflecting aggregation and heterogeneity (Table 1, Figure 2 C3-C5). PdI serves as a means to evaluate the overall uniformity of particle dispersion [16]. When the PdI value is low (≤ 0.05), it indicates a high level of uniform dispersion. On the other hand, PdI values higher than 0.7 mean that the particles in the dispersion are of many different sizes [16]. PdI is also an important factor for figuring out how stable the particle dispersion is, especially when it comes to the possibility of agglomeration happening over time. Our findings indicated PdI values of 0.7 and 1.0 for the non-filtered and filtered samples, respectively (Table 1). These results indicate that SiO_2 particles have a propensity to aggregate. Based on the morphological and size distribution analyses, the functionalization was carried out using the samples prepared under Condition 1, as these exhibited the smallest and most optimal PdI values, indicating good dispersibility.

3.2 FTIR spectroscopy

The FTIR spectra reveal significant differences in the vibrational bands of unmodified SiO_2 nanoparticles compared to SiO_2 nanoparticles functionalized with APTMS (Figure 3).

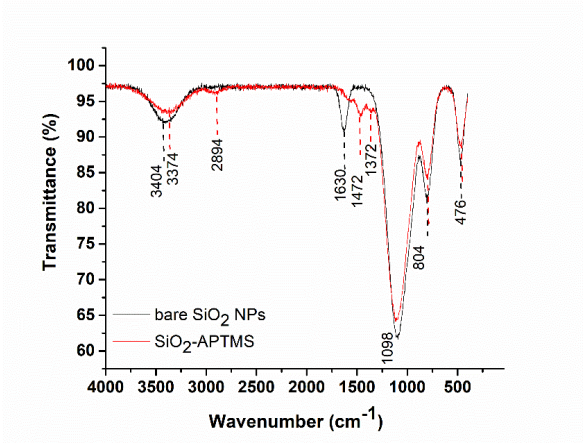

Figure 3. FTIR spectrum of the SiO_2-APTMS

Both spectra demonstrate strong vibrations around 1098 cm^{-1}, 804 cm^{-1}, and 476 cm^{-1}. These bands correspond to the Si–O–Si asymmetric stretching, symmetric stretching, and bending vibrations, respectively, which confirms the silica framework [17]. New characteristic peaks appeared in the functionalized SiO_2–APTMS. In these peaks, the vibration at 2894 cm^{-1} is caused by C–H stretching vibrations of the $–CH_2$ groups, and the peaks around 1630 cm^{-1} and 1472 cm^{-1} are caused by N–H bending and CH_2 scissoring modes from the aminopropyl groups [18]. The broad peak at 3374 cm^{-1} occurs due to the overlapping of O–H stretching vibrations from silanol and adsorbed water and N–H stretching vibrations from the grafted amine groups.

3.3 Quantification of Amine Grafting on SiO_2-APTMS

The ninhydrin test was used to find out how much amine was grafted onto SiO_2-APTMS. At first, ninhydrin reacted with the amine group of APTMS to produce an imine. Figure 4 illustrates the reaction of ninhydrin with a primary amine.

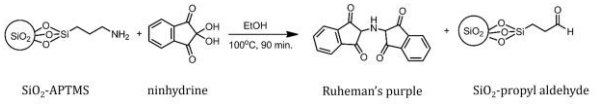

Figure 4. Reaction of ninhydrin with the primary amine groups on SiO_2-APTMS to form Ruhemann's product

First, the amine reacts with ninhydrin to form an imine-type compound. After some condensation steps, a highly conjugated molecule called Ruhemann's purple is formed [19]. This very deep blue-violet chromophore is what causes the color change, which makes it a useful tool for the detection of amines.

The ninhydrin colorimetric test result is summarized in Table 2, which indicates a strong amine presence on the surface of the SiO_2–APTMS.

Table 2. Determination of the amine content using a ninhydrin colorimetric study

No	Unknown sample	Absorbance (λ_{max}: *580 nm*)	Concentration (M)	µmol APTMS/ g SiO_2
1	SiO_2_APTMS	0.981	0.903	684.1

The absorbance value of 0.981 at 580 nm corresponds to a calculated concentration of 0.903 M, which is relatively high. This suggests efficient grafting of aminopropyl groups onto the silica framework. Furthermore, the concentration value was converted to the amount of mol of aminopropyl groups on the silica surface, and the loading amount was found to be 684.1 µmol aminopropyl per gram of SiO_2 nanoparticles.

TG Analysis: The thermal stability of SiO_2-APTMS nanoparticles was evaluated by thermogravimetric analysis, as illustrated in Figure 5. The TGA curve exhibits a multistep weight loss pattern. A first weight loss of approximately 7.7% at approximately 87.5°C occurred due to the desorption of physically adsorbed water and remaining solvents. The second major degradation event occurred at approximately 295°C, resulting in a weight loss of 9.5%, and was associated with the decomposition of organic moieties originating from the 3-aminopropyltrimethoxysilane (APTMS) groups covalently grafted onto the silica surface.

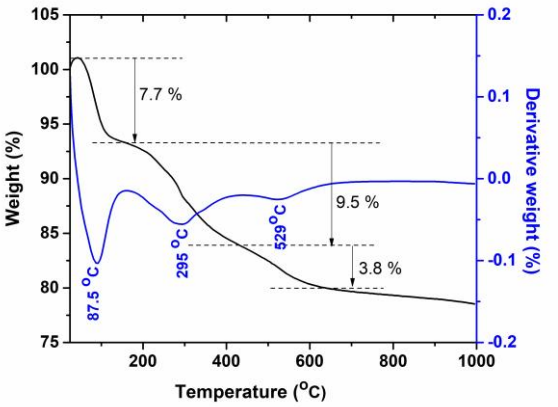

Another weight loss of 3.8% at approximately 529°C can be ascribed to the partial dehydroxylation of the silica particle [20]. After this point, the sample maintains approximately 79% of its initial mass up to 1000°C, confirming the high thermal durability of

the silica framework and providing evidence for the presence of covalently attached organic functionalities (Figure 5). The BET surface area of SiO_2-APTMS was found to be 103 m^2/g, which means that it has a moderately developed porous structure (Table 3). The BJH analysis proved that the total pore volume was 1.55 mL/g, and the BET pore volume was found to be 1.26 mL/g.

Figure 5. TGA curve of the SiO_2-APTMS

Table 3. Quantification of amine loading using the ninhydrin experiment, TG analysis, and surface area of SiO_2-APTMS

Sample	Calculation of amine loading				Surface area, S_{BET} (m^2/g)
	MQA (mol/g)	Surface density_ APTMS (μmol/m^2)	NAM (molecule/nm^2)	Grafting ratio (%)	
Ninhydrin test	$6.84x10^{-4}$	6.64	3.40	7.96	103
TGA data	$1.64 x10^{-3}$	15.9	9.56	19.0	

The quantification in Table 3 demonstrates that both the ninhydrin assay and TGA consistently show that SiO_2 was successfully functionalized with APTMS, but they do so in different ways. From the ninhydrin test, the *MQA* is $6.84x10^{-4}$ mol/g, corresponding to a surface density of 6.64 (μmol/m^2), *NAM* of 3.40 molecules/nm^2, and a weight fraction (W_{ap}) of 7.96%. By contrast, TGA gives a higher *MQA* of $1.64x10^{-3}$ mol/g with *NAM* of 9.56 molecules/nm^2 and W_{ap} of 19%. This discrepancy suggests that TG analysis total organic loading, while ninhydrin selectively detects accessible amine groups.

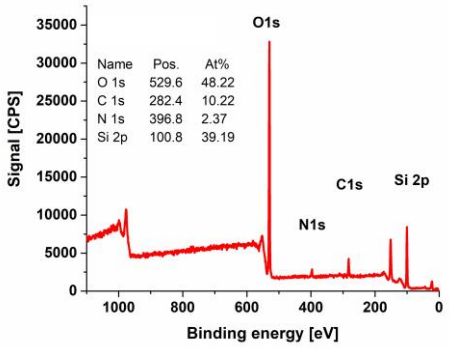

Figure 6. XPS of the SiO_2-APTMS

XPS Analysis: In order to identify the binding energies of the ligand molecule onto he silica surface and determine the atomic percentage of the composition, XPS analysis was utilized [21]. According to that, the XPS spectrum revealed that 48.22% of oxygen (O), 39.19% of silicon (Si), 10.22 % of carbon (C), and 2.37% of nitrogen (N) have been present in the nanoparticle (Figure 6). From these values, the experimental molar ratio of C/N was calculated to be 4.31. In comparison, the theoretical ratio of C/N for the molecular structure of $C_3H_8NSiO_3$ (excluding hydrogen, which cannot be detected by XPS) is 3.00. The mol ratio of C/N in the XPS result was found to be higher compared to the theoretical calculation, which could be attributed to the contribution of adventitious carbon that is typically present on sample surfaces. On the other hand, one other important molar ratio of O/Si. In XPS analysis, the O/Si ratio was found to be 1.23, whereas O/Si was 3.00 in the theoretical calculation, which yielded a significantly lower ratio than the theoretical ratio.

This reveals that the XPS signal is dominated by contributions from the SiO_2 nanoparticle, while the thin aminopropyl overlayer contributes a smaller fraction to the overall composition. The relatively low nitrogen content further supports the conclusion that only a small number of APTMS molecules are attached to the SiO_2 surface, which was also supported by the grafting ratio obtained from TG analysis and ninhydrin tests.

3.4 Adsorption study

In the present study, the interaction behavior of La^{3+}, Nd^{3+}, Dy^{3+}, and Er^{3+} ions with SiO_2–APTMS nanoparticles was systematically examined. The influence of contact duration on ion uptake was evaluated, and the corresponding results are illustrated in Figure 7.

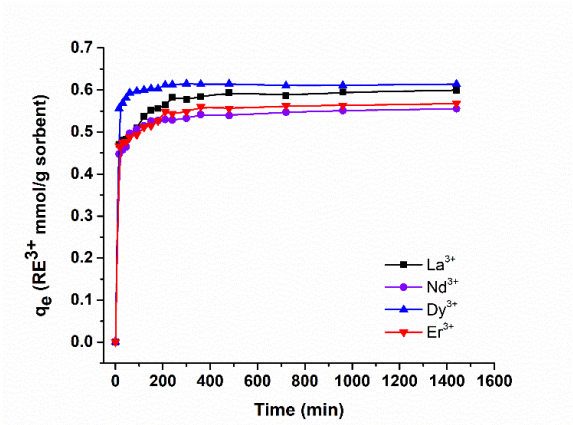

Figure 7. Adsorption kinetics of La^{3+}, Nd^{3+}, Dy^{3+}, and Er^{3+} ions onto the sorbent, showing the variation of equilibrium adsorption capacity (q_{eq}, $mmol{\cdot}g^{-1}$) with contact time.

All of the rare earth ions demonstrated a rapid initial uptake within the first 100 minutes, which can be attributed to the affinity of the free amine groups on the active surface sites (Figure 7). Thereafter, the rate of the adsorption gradually decreased until reaching the equilibrium at around 200 minutes. Dy^{3+} exhibited the highest uptake with 0.63 $mmol.g^{-1}$ which is followed by La^{3+}, Nd^{3+}, and Er^{3+} reaching values in the range of 0.56–0.60 $mmol.g^{-1}$. The corresponded mg/g values were given in Table 4. This proposes a moderate selectivity of the SiO_2-APTMS towards Dy^{3+}, likely due to its favorable ionic property and binding affinity.

Table 4. Isolation of rare earths using ligand functionalized sorbents

Sorbent	Adsorption capacity (mg/g)	Ref
PCDP-M-SHM	Y^{3+}:62.3; Nd^{3+}:49.2; Eu^{3+}:51.2; Gd:40.9	[22]
APTES-C3-PAN	La^{3+}:21.5; Sc^{3+}:13.4; Y^{3+}:18.4	[23]
MSN-2NH-2COOH	Dy^{3+}: 32.9	[24]
GO-PER	La^{3+}: 27.92; Y^{3+}: 30.44, Nd^{3+}: 43.2; Er^{3+}: 48.08; Yb^{3+}: 52.4	[25]
FCCD	Dy^{3+}: 28.3; Nd^{3+}: 27.1; Er^{3+}: 30.6	[26]
SiO2-APTMS	La^{3+}:83.3; Nd^{3+}: 80.7; Dy^{3+}: 102.4; Er^{3+}: 95.4	our study

Numerous investigations have demonstrated the effectiveness of functionalized sorbent materials for the immobilization of rare earth ions. Nkinahamira et al. developed a β-cyclodextrin–based hybrid composite (PCDP/Fe_3O_4) modified with silica doped by 2-ethylhexyl phosphonic acid mono-2-ethylhexyl (PC88A). The resulting material, denoted as PCDP-M-SHM, showed notable uptake performance, with maximum retention values of 62.3 mg g^{-1} for Y^{3+}, 49.2 mg g^{-1} for Nd^{3+}, 51.2 mg g^{-1} for Eu^{3+}, and 40.9 mg g^{-1} for Gd^{3+} [22]. Ramasamy et al. reported the fabrication of polyacrylonitrile-modified mesostructured sorbents derived from APTES-functionalized silica combined with high-molecular-weight chitosan. These materials exhibited metal ion affinities of 21.5 mg g^{-1} for La^{3+}, 13.4 mg g^{-1} for Sc^{3+}, and 18.4 mg g^{-1} for Y^{3+} [23]. Kaneko et al. synthesized mesoporous silica nanoparticles bearing amine and carboxyl functionalities and evaluated their interaction with Dy^{3+}, achieving a maximum binding capacity of 32.9 mg g^{-1} [24]. In another study, Liao et al. engineered three-dimensional graphene oxide–pentaerythritol (GO-PER) architectures enriched with oxygen-based surface moieties, including carboxyl, hydroxyl, carbonyl, and epoxy groups. These composites demonstrated substantial metal capture efficiencies, reaching 27.92 mg g^{-1} for La^{3+}, 30.44 mg g^{-1} for Y^{3+}, 43.2 mg g^{-1} for Nd^{3+}, 48.08 mg g^{-1} for Er^{3+}, and 52.4 mg g^{-1} for Yb^{3+} [25]. Additionally, Liu et al. introduced a magnetic bio-based material, Fe_3O_4-C18-chitosan-DETA (FCCD), synthesized through a surface deposition followed by stepwise grafting strategy. Under optimal conditions (pH 7.0, 25 °C), the composite achieved retention capacities of approximately 28.3 mg g^{-1} for Dy^{3+}, 27.1 mg g^{-1} for Nd^{3+}, and 30.6 mg g^{-1} for Er^{3+} [26]. The literature examples discussed above, together with the findings of the present study, are summarized in Table 4.

4. Conclusion

In this study, SiO_2 nanoparticles were synthesized in high yields under various reaction conditions, and particle sizes ranging from ~12 to 111 nm were obtained, as confirmed by TEM analysis. DLS measurements also indicated particle aggregation behavior with high polydispersity index values, highlighting the effect of dispersion stability on particle size distribution. Surface functionalization of silica nanoparticles with APTMS was confirmed by FTIR, which showed the appearance of characteristic propyl chain and primary amine vibration bands next to the Si–O–Si framework peaks. Quantification of the surface grafting using ninhydrin assay, TGA, and XPS showed efficient integration of aminopropyl groups; TGA indicated total organic content, while ninhydrin selectively identified accessible amines. XPS provided additional confirmation by the detection of nitrogen and carbon signals consistent with the APTMS modification. Finally, adsorption experiments with rare-earth ions showed a rapid sorption within 100 min and equilibrium in approximately 200 min, with Dy^{3+} having the highest affinity. These results demonstrate the successful preparation of thermally stable amine-functionalized silica nanoparticles with potential application in the capture and recovery of rare earth ions.

Acknowledgment

This study was funded by the TUBITAK 2531 program under Grant/Project No 221N430.

Declaration of Ethical Code

In this study, we undertake that all the rules required to be followed within the scope of the "Higher Education Institutions Scientific Research and Publication Ethics Directive" are complied with, and that none of the actions stated under the heading "Actions Against Scientific Research and Publication Ethics" are not carried out.

References

[1] Nanyl A.A. , Abd-Elhamid A.I. , Aly A.A., Bräse S. 2022. Recent progress in the application of silica-based nanoparticles, RSC Advances, 22, 13706-13726.

[2] Ghodrati M., Mousavi-Kamazani M., Bahrami Z. 2023. Synthesis of superhydrophobic coatings based on silica nanostructure modified with organosilane compounds by sol-gel method for glass surfaces, Scientific Reports, 13, 548.

[3] Miller P.J, Shantz D.F. 2020. Covalently functionalized uniform amino-silica nanoparticles. Synthesis and validation of amine group accessibility and stability", Nanoscale Adv, 2, 860-868.

[4] Singh V., Mandal T., Mishra S.R., Singh A., Khare P. 2024. Development of amine-functionalized fluorescent silica nanoparticles from coal fly ash as a sustainable source for nanofertilizer, Scientific Reports, 14, 3069.

[5] Chen Y., Zhang Y. 2011. Fluorescent quantification of amino groups on silica nanoparticle surfaces, Bioanal. Chem., 399, 2503–2509.

[6] Sun Y., Kunc F., Balhara V., Coleman B., Kodra O., Raza M., Chen M., Brinkmann A., Lopinski G.P., Johnson L.J. 2019. Quantification of amine functional groups on silica nanoparticles: a multi-method approach, Nanoscale Adv., 1, 1598–1607.

[7] Dev R.K., Yadav S.N, Magar N., Ghimire S., Koirala M., Giri R., Das A.K., Sah S.K., Gardas R.L., Bhattarai A. 2025. Recovery of Rare Earth Elements (REEs) From Different Sources of E-Waste and Their Potential Applications: A Focused Review, Geological J., 60, 1775-1798.

[8] Liu J., Lu X., Li Q., Xue Z., Zhang Q., Zhao Y., Wu G., Ma B., Xia W. 2025. Separation and recovery of low concentration rare earth elements from wastewater using a porous magnetic composite of carboxymethyl-β-cyclodextrin and silica, Separation and Purification Tech., 372, 133313.

[9] Hu Y., Castro L.C.M., Drouin E., Florek J., Kahlig H., Lariviere D., Kleitz F., Fontaine F.G. 2019. Size-selective separation of rare earth elements using functionalized mesoporous silica materials, ACS Appl. Mater. Interfaces, 11, 23681–23691.

[10] Ramasamy D.L., Khan S., Repo E., Sillanpää M. 2017. Synthesis of mesoporous amine and non-amine functionalized silica gels for the application of rare earth elements (REE) recovery from wastewater: understanding the role of pH, temperature, calcination, and mechanism in light REE and heavy REE separation, Chem. Eng. J., 322, 56–65.

[11] Vardanyan A., Guillon A., Budnyak T., Saisenbaeva G. 2022. Tailoring nanoadsorbent surfaces: separation of rare earths and late transition metals in recycling of magnet materials, Nanomaterials, 12, 974.

[12] Fernandes R.S., Raimundo I.M., Pimentel M.F. 2019. Revising the synthesis of Stöber silica nanoparticles: a multivariate assessment study on the effects of reaction parameters on particle size, Colloids Surf. A: Physicochem. Eng. Aspects, 577, 1–7.

[13] Kunc F., Balhara V., Brinkmann A., Sun Y., Leek D.M., Johnston L.J. 2018. Quantification and stability determination of surface amine groups on silica nanoparticles using solution NMR, Anal. Chem., 90, 13322–13330.

[14] Sun Y., Kunc F., Balhara V., Coleman B., Kodra O., Raza M., Chen M., Brinkmann A., Lopinski G.P., Johnston L.J. 2019. Quantification of amine functional groups on silica nanoparticles: a multi-method approach, Nanoscale Adv., 1, 1598–1607.

[15] Lu H.T. 2013. Synthesis and characterization of amino-functionalized silica nanoparticles, Colloid Journal, 75, 311–318.

[16] Clayton K.N., Salameh J.W., Wereley S.T., Kinzer-Ursem T.L. 2016. Physical characterization of nanoparticle size and surface modification using particle scattering diffusometry, Biomicrofluidics, 21, 054107.

[17] Yemin M.N., Sultana M., Siddika A., Tabassum S., Ullah S.M., Bashar M.S. 2022. Structural, optical and morphological characterization of silica nanoparticles prepared by sol–gel process, J. Turkish Chem. Soc. Sec. A: Chem., 9, 1323–1334.

[18] Petreanu I., Niculescu V.C., Enache S., Iacob C., Teodorescu M. 2022. Structural characterization of silica and amino-silica nanoparticles by Fourier transform infrared (FTIR) and Raman spectroscopy, Analytical Lett., 56, 390–403.

[19] Friedman M. 2004. Application of ninhydrin reaction for analysis of amino acids, peptides, and proteins in agricultural and biomedical sciences, J. Agric. Food Chem., 52, 385–406.

[20] Yu M., Qiao X., Dong X., Kang S. 2018. Effect of particle modification on the shear thickening behaviors of suspensions of silica nanoparticles in PEG, Colloid Polym. Sci., 296, 1767–1776.

[21] Beyler-Cigil A. 2020. Preparation, characterization, and adsorption into aqueous solutions of polyethyleneimine-coated silica nanoparticles, J. Turkish Chem. Soc. Sec. A: Chem., 7, 883–892.

[22] Nkinahamira F., Alsbaiee A., Wang Y., Yang X., Chen T.Y., Cao M., Feng M., Sun Q., Yu C.P. 2021. Recovery and purification of rare earth elements from wastewater and sludge using a porous magnetic composite β-cyclodextrin and silica doped with PC88A, Seperation and Purification Tech., 266, 118589.

[23] Ramasamy D.L. Wojtus A., Repo E., Kalliola S., Srivastava V., Sillanpää M. 2017. Ligand immobilized novel hybrid adsorbents for rare earth elements (REE) removal from waste water: Assessing the feasibility of using APTES functionalized silica in the hybridization process with chitosan, Chem Eng. J., 330, 1370-1379.

[24] Kaneko T., Nagata F., Kugimiya S., Kato K. 2018. Optimization of carboxy-functionalized mesoporous silica for the selective adsorption of dysprosium, J. Enviro. Chem. Eng. 6, 5990-5998.

[25] Liao C., Zhao X.R., Jiang X.Y., Teng J., Yu J.G. 2020. Hydrothermal fabrication of novel three-dimentional graphene oxide pentaerythritol composites with abundant oxygen-containing groups as efficient adsorbents, Microchem. J., 152, 104288.

[26] Liu E., Zheng X., Xu X., Zhang F., Liu E., Wang Y., Li C., Yan Y. 2017. Preparation of Diethylenetriamine-modified magnetic chitosan nanoparticles for adsorption of rare-earth metal ions, New. J. Chem., 41, 7739-7750.